Comment on "Bottom-Up Graphene-Nanoribbon Fabrication Reveals Chiral Edges and Enantioselectivity"

■ In a recent paper,[1] Han *et al.* published a study on the formation of graphene nanoribbons (GNRs) on Cu(111) from 10-10′-dibromo-9-9′-byanthracene (DBBA) precursor molecules. A very similar investigation was reported by us several months earlier,[2] but there is no reference to our work by the authors of ref 1. More importantly, they come to very different conclusions regarding the process of formation of the GNRs and their final structure. For this reason, we find it necessary to clarify and to give further support for our original interpretation, thereby questioning several key conclusions in ref 1.

The authors of ref 1 declare that the surface atomic structure of Cu(111) and its catalytic properties result in polymerization of DBBA precursors into (3,1)-chiral GNRs instead of 7-armchair GNRs (7-AGNRs) as observed on Au(111)[3] and Ag(111).[4] This contradicts our previous conclusion for GNRs on Cu(111).[2] The authors describe the results of three STM experiments: (i) after DBBA/Cu(111) deposition at room temperature (RT); (ii) after annealing from RT to 200 °C; (iii) after annealing to 500 °C. In the following, we consider each of the experimental steps in some detail and raise questions based on our own results that cast doubt on the proposed model.

For the correct comparison of results in refs 1 and 2, it is essential to provide more detail of our sample preparation procedures because the kinetics of the growth process could influence the final structure of the nanoribbons. In our experiments, the DBBA molecules were deposited from a homemade Knudsen cell with a Ta crucible and a K-type thermocouple (ThC) spot-welded directly to the outer wall of the crucible. Before deposition, the molecules were outgassed for several hours in ultrahigh vacuum (UHV) at a temperature of approximately 100 °C. The molecules were then deposited on a clean Cu(111) substrate maintained at RT in UHV (the pressure during deposition was about 1×10^{-9} mbar, and the base pressure in the preparation chamber was 1×10^{-10} mbar). The deposition time (on the order of 1 h) was selected to ensure that the amount of deposited material did not exceed a monolayer. The Cu(111) crystal was heated by a filament at the back; for annealing to temperatures above 300 °C, e-beam heating was used. The annealing temperature was monitored with a K-type ThC in direct contact with the side of the Cu(111) crystal and thus provided a direct measurement of the crystal temperature. At temperatures higher than 400 °C, a pyrometer was also used to confirm the sample temperature. The difference in the temperature values measured by the ThC and the pyrometer was never more than 25 °C. After measurements performed at RT, the sample was heated at a rate of 10−15 °C/min and annealed stepwise at 100, 150, 200, and 250 °C for 15 min at each step. Higher temperatures (up to 750 °C) were also used to study the decomposition of the GNRs. After each annealing step, the sample was cooled to RT for scanning tunneling microscopy (STM) and X-ray photoelectron spectroscopy measurements; some STM measurements were performed at −160 °C. The STM experiments were reproduced in two different STM systems with two different Cu(111) crystals.

According to Han *et al.*, at the first step, the DBBA molecules remain intact (not debrominated) on Cu(111) at RT and form molecular chains through a $\pi-\pi$ stacking interaction, as shown in Figure 2 of ref 1. However, in ref 2, we used photoelectron and X-ray absorption spectroscopy of the C 1s and Br 3d core levels to obtain detailed information on the adsorption of DBBA on different substrates. On Au(111), we find spectra that are consistent with nondissociative adsorption. On Cu(111), on the other hand, the spectra clearly show that the DBBA molecules adsorb dissociatively and that complete surface-assisted dehalogenation occurs below RT. In contrast, in ref 1, the authors claim that the debromination of DBBA/Cu(111) takes place at temperatures in excess of 200 °C. This is higher than the debromination temperature of DBBA on inert Au(111), where previously it has been shown that the dehalogenation reaction starts at about 120 °C and is completed at 200 °C.[2,5] In turn, debromination at RT implies the formation of dangling bonds, which are very active and tend to interact with the Cu(111) surface, as confirmed by our spectroscopic data (see Figures 5−8 in ref 2). In particular, the low-energy shoulder at 283.0 eV in the C 1s photoemission spectrum (Figure 7 in ref 2) was associated with the Br-deprived C atoms forming C−Cu bonds. Thus, the molecular chain model, suggested in ref 1 as an explanation for the experimental STM image of DBBA/Cu(111) observed at RT, is not consistent with these observations. Nevertheless, our STM images obtained at RT (Figure 1a), are in agreement with those presented by Han *et al.* (Figure 1b,c in ref 1). The long "chain-like" structures with the periodic bright protrusions on either side of the central axis of the chain can be clearly seen at RT (Figure 1a). However, the chain-like structures observed upon annealing at 100 °C are visibly different (Figure 1b). As can be seen from the insets in Figure 1a,b, the periodicity along the DBBA chain at RT (1.25 nm) is significantly larger than that of the chains formed at 100 °C (0.85 nm), as additionally illustrated in Figure 1 by the profiles taken along four bright protrusions parallel to the chain axis for both cases. The measured value of 0.85 nm for the period of chains formed upon annealing at 100 °C is in perfect agreement with the previously reported value measured for polymer chains on Au(111)[3] and is fully consistent with the proposed structural model (*i.e.*, individual debrominated DBBA molecules linked by the covalent C−C bonds along the chain axis). When the spectroscopic evidence mentioned above for the interaction between the debrominated DBBA molecule and the Cu atoms at RT is taken into account, it is proposed that Figure 1 in ref 1 and Figure 1a herein illustrate organometallic surface-stabilized chains, consisting of debrominated DBBA molecules bonded at each end to the Cu substrate or Cu adatoms. Similar structures have

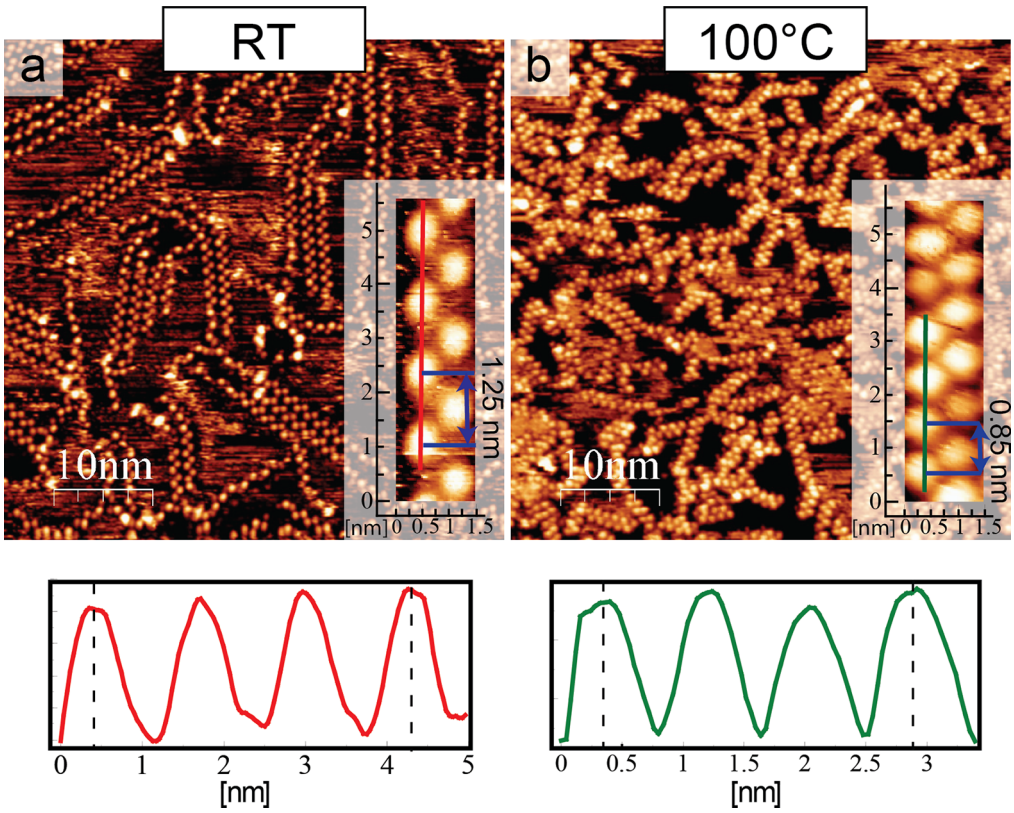

Figure 1. 50 × 50 nm^2 STM images of DBBA chains on Cu(111) at RT (a) and polymer chains obtained after annealing to 100 °C (b). The insets in (a) and (b) show high-resolution images of a surface-confined DBBA chain at RT and a polymer chain at 100 °C, with the measured distance between protrusions. The line profiles are taken along the corresponding red and green lines on the insets and indicate the difference in periodicity of the structures obtained at RT (red profile) and 100 °C (green profile). Tunneling parameters: (a) −0.61 V/0.1 nA, (b) +2.35 V/0.5 nA.

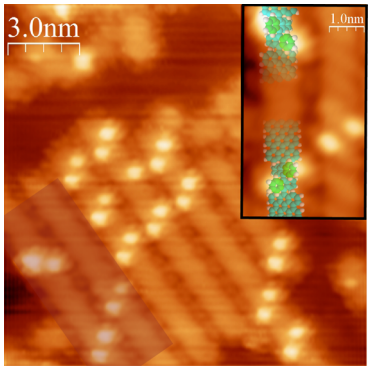

Figure 2. 15 × 15 nm^2 STM image showing under-annealed 7-AGNRs on Cu(111) obtained after heating at 200 °C. The inset shows an enlarged image of two GNRs (highlighted with a transparent rectangle in the main image) and a corresponding ball and stick model. In this model, the aromatic rings pointing upward are colored bright green. The circular features around and between the GNRs are attributed to detached Br atoms. The image was taken at 110 K; V_s = −0.27 V, I_t = 330 pA.

been reported in numerous studies as intermediates in on-surface polymerization reactions (Ullmann coupling).[6] Although the exact geometry of debrominated DBBA on Cu(111) at RT remains to be established, the bright protrusions on both sides of the axis within such surface-stabilized metal−organic chains appear to have the same nature as for the polymer chains obtained at 100 °C and is due to the opposite tilt of the adjacent anthracene units. The comparison performed in Figure 1 clearly proves that polymer chain formation is a necessary step in the GNR growth process.

Under certain tunneling conditions, images of the chain-like structures at RT reveal adatoms, sitting at the edges of chains (see Figure S6a in ref 1), which are also visible in images of the polymer chains at 100 °C (Figure 1b). These atoms are assumed to be Br adatoms, resulting from DBBA debromination at RT. Interestingly, the Br adatoms are not visible in the case of polyanthracene chains on Au(111) because they are hidden under the twisted anthracene units.[7] We believe that in the case of Cu(111) the stronger interaction between the on-surface molecular structure and the substrate can push Br atoms away from the center of bianthryl units, making them visible in the STM images. The Br atoms can be dispersed by high-bias imaging (Figure S2 in ref 1). This fact was interpreted by Han *et al.*[1] as a tip-induced dehalogenation. Most likely, the tip-induced reduction in the apparent height observed in Figure S2 of ref 1 results from the local polymerization accompanied by partial internal dehydrogenation

inside the polymer segment of the metal−organic chain.

At step (ii), further annealing at 200 °C took place. According to the STM data in ref 1, this results in the formation of 2D islands composed of single-crystal DBBA domains. However, core-level spectroscopy provides a different interpretation.[2] On the active Cu(111) substrate, the dehydrogenation inside the polyanthracene chains begins at temperatures of around 150 °C, and by 250 °C, flat GNRs are formed. This is a much lower temperature than on the inert Au(111) substrate, where the GNRs are formed at 400 °C.[2,3] To verify our model, we have performed an STM study of the intermediate stage of the GNR formation on Cu(111) after annealing to 200 °C, where the dehydrogenation reaction is incomplete. An STM image of these "under-annealed" GNRs is shown in Figure 2. Apparently, the GNRs contain pairs of bright protrusions analogous to those observed in the polyanthracene chains at 100 °C. As the annealing temperature was not high enough, the cyclodehydrogenation process inside the polyanthracene chain was not completed, leaving some of the anthracene units tilted with respect to the axis of the flat GNRs. This is schematically shown in the inset of Figure 2. It is possible to obtain oppositely tilted pairs of anthracene units incorporated into the same GNR or, sometimes, even individual (not paired) protrusions at places where dehydrogenation was completed only on one side of the precursor molecule. These observations cannot be explained in the framework of the "molecular chain" model suggested by Han *et al.* (see Figure 5 in ref 1), where the anthracene lobes in all of the DBBA units are tilted in the same way, thus excluding the possibility of obtaining an image similar to that shown in Figure 2. Further annealing of the sample at 250 °C leads to the disappearance of the bright protrusions and results in the formation of flat GNRs, identical to those obtained in ref 2.

At step (iii), the authors of ref 1 claim that annealing to 500 °C leads to the formation of GNRs on Cu(111). However, as discussed above, GNRs are readily formed at 250 °C on this surface. Moreover, further annealing of GNRs/Cu(111) to temperatures higher than 400 °C results in the decomposition and amorphization, as can be seen in the C 1s photoemission spectra in ref 2. To provide more evidence, we show in Figure 3 an STM image of the decomposed GNRs on Cu(111) after annealing to 420 °C. Irregularly shaped islands of decomposed material surrounding a flat central region are observed accompanied by trenches etched into the surface. It is proposed that as the GNRs decompose there is a mass transport from the underlying substrate resulting in trenches that are comparable in width to the GNRs, ∼2 nm. The trenches appear to form along regions of the surface occupied by the GNRs, while line profiles across the trenches show that they

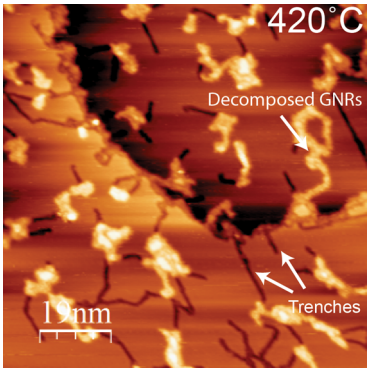

Figure 3. 95 × 95 nm^2 STM image showing decomposed GNRs on Cu(111) obtained after annealing at 420 °C. Image parameters: V_s = 1.00 V, I_t = 100 pA.

are one Cu(111) layer in depth, ∼0.2 nm. Further annealing of this surface eventually results in the formation of small single-layer graphene islands at temperatures in excess of 700 °C.[2] The formation of trenches has also been observed upon decomposition of H_2-tetrabromophenyl porphyrin and Ni-tetrabromophenyl porphyrin molecules on Cu(111).[8] It is noted that in all cases Br is present in the molecule and may play a role in the creation of the trenches through the formation of CuBr moieties on the surface and their subsequent desorption at temperatures above 400 °C. The resulting vacancies created on the Cu surface may then act as nucleation sites for the decomposition of the GNRs.

Now, let us discuss the structure of the GNRs. Han *et al.* find an exponentially decreasing length distribution of the GNRs (see Figure 4 in ref 1), where the majority of the structures are very short, below 2 nm, which implies a length of only one or two DBBA molecules. For this reason, most of them can hardly be called GNRs. The fraction of longer GNRs present is very small, and very few of them have lengths in excess of 6 nm. On the basis of these data, the authors made conclusions about the non-diffusion-controlled nature of GNR growth. This is in stark contrast to our finding that most of the GNRs on Cu(111) have lengths of between 10 and 20 nm.[2] In Figure 4, we show the typical length distributions for GNRs/Cu(111) and GNRs/Au(111), as obtained from the data published in ref 2. It is clear that the length distribution of GNRs on Cu(111) is very different from the exponentially decaying distribution found in ref 1. Our distribution for Au(111) is furthermore in excellent agreement with the one published in ref 3. As illustrated in Figure 4, the distributions for Cu(111) and Au(111) are indeed qualitatively similar and indirectly point to the same growth mechanism of GNRs *via* polymer chain formation. Therefore, the conclusion about the large impact of different diffusion rates on Cu(111) and Au(111) on the growth mechanism of GNRs is questionable. On the other hand, the length distribution can easily

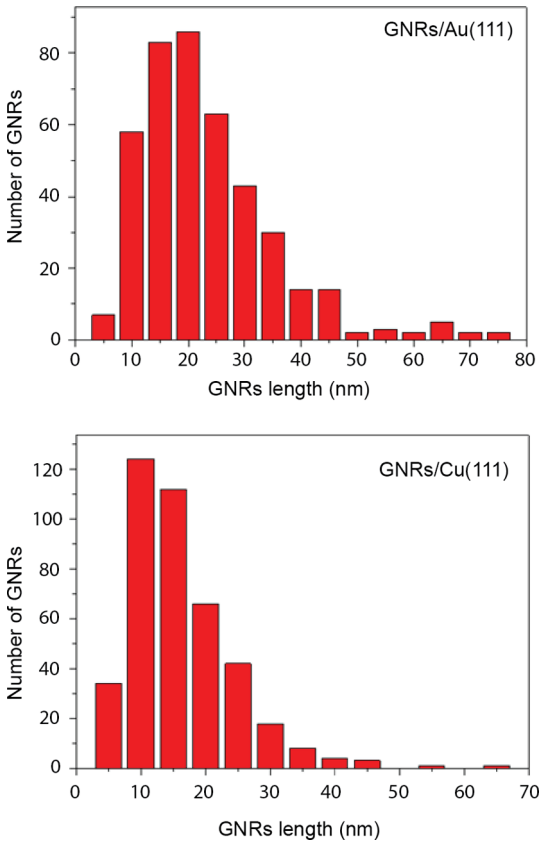

Figure 4. Length distributions of GNRs/Au(111) and GNRs/Cu(111) obtained from the STM data in ref 2.

be affected by the growth conditions. As discussed above, in our experiments, we always used low heating rates and rather long annealing times to reduce the effect of kinetics-related disorder on the resulting structure of the GNRs. It is possible that the distribution presented in ref 1 is characteristic of the growth determined by conditions further from thermodynamic equilibrium. In particular, too fast annealing could lead to the activation of internal dehydrogenation process inside individual molecules prior to the formation of covalently bonded polymer chains resulting in a large number of disoriented flat single-molecule derivatives. This could explain such a small fraction of ribbons with the length exceeding 5 nm observed in ref 1.

Nevertheless, despite all of the inconsistencies, our high-resolution STM images do reveal, under certain tunneling conditions, a similar zigzag shape of the GNR edges as those presented in Figure 3b of ref 1 (in particular, this can be seen in Figure 2 above). On the basis of such an edge profile and the suggested growth model, Han *et al.* have concluded that the resulting nanoribbons have a (3,1) chiral edge configuration. On the other hand, taking into account the inconsistency of the GNRs' growth mechanism proposed in ref 1, the (3,1) chiral edge structure is problematic as it is unclear how (3,1)-GNRs can be formed from covalently bonded polyanthracene chains *via* cyclodehydrogenation. Moreover, according to the structure suggested by the authors, the (3,1)-GNRs are hydrogen-terminated (Figure 3c in ref 1), while the proposed formation mechanism (Figure 5 in ref 1) ignores the presence of the dangling bonds, which would appear on both sides of the GNRs after debromination. In this connection, it is unclear what is the role of Br atoms in precursor molecules for the (3,1)-GNR formation proposed by Han *et al.*, as the dangling bonds caused by debromination are supposed to not be engaged in the polymerization process. For example, it would be interesting to know whether the use of 9-9′-bianthracene molecules ($C_{28}H_{18}$), where Br atoms of DBBA are replaced by H atoms, is believed to result in the same chiral (3,1)-GNR structure as the one shown in Figure 5 of ref 1.

Although the structure of the GNRs on Cu(111) is not entirely clear, we can with certainty propose that they are 7-AGNRs. The edge structure observed in some STM images may be attributed to several factors. First, it could be due to the effect of regularly situated Br adatoms surrounding the GNR on the LDOS distribution and/or on the STM imaging conditions. Indeed, unlike Figure 3c of ref 1, in Figure 2, Br atoms can be seen both between the GNRs and surrounding the free edges of GNRs, thus modulating the apparent structure on both sides of the GNRs. A similar effect was observed in STM images from metal−organic chains formed after deposition of diiodobenzene molecules on Cu(110) (see Figure 1 in ref 9). Second, the GNRs interact strongly with the Cu(111) surface, which leads to an alignment of GNRs/Cu(111) along six equivalent directions with respect to the Cu(111) surface, as seen in both refs 2 and 1. Therefore, the lattice mismatch between the GNR and Cu(111) surface in the GNR growth direction may result in a periodic pattern of chemically nonequivalent regions due to the different strength of ribbon−substrate interaction along the GNR. In turn, this can lead to a periodic modulation of the GNR electronic structure and geometry reflected in the STM images.

In conclusion, we have carefully considered the results published by Han *et al.*[1] in the light of our previously published results[2] for the growth of GNRs on Cu(111). The findings in these two publications are very different. As discussed in detail in this comment, we conclude that our original proposals for the structure and properties of polyanthracene chains and GNRs on Cu(111) reported in ref 2 are well-supported and correct: (i) the debromination of the DBBA molecules on Cu(111) is completed below RT; (ii) a necessary intermediate stage in the quasi-equilibrium growth of GNRs is the formation of polyanthracene chains at 100 °C; (iii) the structure of the resulting nanoribbons is identical to the 7-AGNRs formed on Au(111).

REFERENCES AND NOTES

1. Han, P.; Akagi, K.; Canova, F. F.; Mutoh, H.; Shiraki, S.; Iwaya, K.; Weiss, P. S.; Asao, N.; Hitosugi, T. Bottom-Up Graphene-Nanoribbon Fabrication Reveals Chiral Edges and Enantioselectivity. *ACS Nano* **2014**, *8*, 9181–9187.
2. Simonov, K. A.; Vinogradov, N. A.; Vinogradov, A. S.; Generalov, A. V.; Zagrebina, E. M.; Mårtensson, N.; Cafolla, A. A.; Carpy, T.; Cunniffe, J. P.; Preobrajenski, A. B. Effect of Substrate Chemistry on the Bottom-Up Fabrication of Graphene Nanoribbons: Combined Core-Level Spectroscopy and STM Study. *J. Phys. Chem. C* **2014**, *118*, 125352–12540.
3. Cai, J.; Ruffieux, P.; Jaafar, R.; Bieri, M.; Braun, T.; Blankenburg, S.; Muoth, M.; Seitsonen, A. P.; Saleh, M.; Feng, X. L.; Müllen, K.; Fasel, R. Atomically Precise Bottom-Up Fabrication of Graphene Nanoribbons. *Nature* **2010**, *466*, 470–473.
4. Huang, H.; Wei, D.; Sun, J.; Wong, S. L.; Feng, Y. P.; Neto, A. H. C.; Wee, A. T. S. Spatially Resolved Electronic Structures of Atomically Precise Armchair Graphene Nanoribbons. *Sci. Rep.* **2012**, *2*, 983.
5. Batra, A.; Cvetko, D.; Kladnik, G.; Adak, O.; Cardoso, C.; Ferretti, A.; Prezzi, D.; Molinari, E.; Morgante, A.; Venkataraman, L. Probing the Mechanism for Graphene Nanoribbon Formation on Gold Surfaces Through X-ray Spectroscopy. *Chem. Sci.* **2014**, *5*, 4419–4423.
6. Fan, Q.; Wang, H.; Han, Y.; Zhu, J.; Kuttner, J.; Hilt, G.; Gottfried, J. M. Surface-Assisted Formation, Assembly, and Dynamics of Planar Organometallic Macrocycles and Zigzag Shaped Polymer Chains with C−Cu−C Bonds. *ACS Nano* **2014**, *8*, 709–718.
7. Bronner, C.; Björk, J.; Tegeder, P. Tracking and Removing Br during the On-Surface Synthesis of Graphene Nanoribbon. *J. Phys. Chem. C* **2015**, *119*, 486–493.
8. Doyle, C. An Investigation of the Structural and Electronic Properties of Covalently Bonded Molecular Networks on Metal Surfaces Formed through Debromination Reactions; Ph.D. Thesis, Dublin City University, Ireland, 2013.
9. Lipton-Duffin, J. A.; Ivasenko, O.; Perepichka, D. F.; Rosei, F. Synthesis of Polyphenylene Molecular Wires by Surface-Confined Polymerization. *Small* **2009**, *5*, 592–297.

Konstantin A. Simonov,[†,‡,§] Nikolay A. Vinogradov,[†,‡,#] Alexander S. Vinogradov,[§] Alexander V. Generalov,[‡,§] Elena M. Zagrebina,[§] Nils Mårtensson,[†] Attilio A. Cafolla,[∥] Thomas Carpy,[∥] John P. Cunniffe,[∥] and Alexei B. Preobrajenski[*,‡]

[†]Department of Physics and Astronomy, Uppsala University, Box 516, 75120 Uppsala, Sweden

[‡]MAX IV, Lund University, Box 118, 22100 Lund, Sweden

[§]V.A. Fock Institute of Physics, St. Petersburg State University, 198504 St. Petersburg, Russia

[∥]School of Physical Sciences, Dublin City University, Dublin 9, Ireland

[#]Present address: Synchrotron Radiation Facility, 6 Rue Jules Horowitz, B.P. 220, FR-38043 Grenoble Cedex, France.

*Address correspondence to alexei.preobrajenski@maxlab.lu.se.

Received for review November 11, 2014

Published online April 28, 2015
10.1021/nn506439a